Journal of Turbulence
Volume 7, No. 51, 2006

Taylor & Francis
Taylor & Francis Group

Energy transfers in forced MHD turbulence

DANIELE CARATI*†, OLIVIER DEBLIQUY†, BERNARD KNAEPEN†,
BOGDAN TEACA‡ and MAHENDRA VERMA§

†Statistical and Plasma Physics, Université Libre de Bruxelles, Campus Plaine, CP 231,
B-1050 Brussels, Belgium
‡Faculty of Physics, University of Craiova, 13 A.I. Cuza Street, 200585 Craiova, Romania
§Department of Physics, I.I.T. Kanpur, Kanpur 208016, India

The energy cascade in magnetohydrodynamics is studied using high resolution direct numerical simulations of forced isotropic turbulence. The magnetic Prandtl number is unity and the large scale forcing is a function of the velocity that injects a constant rate of energy without generating a mean flow. A shell decomposition of the velocity and magnetic fields is proposed and is extended to the Elsässer variables. The analysis of energy exchanges between these shell variables shows that the velocity and magnetic energy cascades are mainly local and forward, though non-local energy transfer does exist between the large, forced, velocity scales and the small magnetic structures. The possibility of splitting the shell-to-shell energy transfer into forward and backward contributions is also discussed.

Keywords: Direct numerical simulation; Homogeneous turbulence; Isotropic turbulence; Turbulence modelling; Subgrid scale

1. Introduction

The study of the nonlinear interactions in fluid turbulence has long been an active subject of research [1–4]. The motivation for such studies is of course to improve the understanding of the physics of turbulence and, more specifically, of the mechanism(s) of energy transfer from the large, geometry-dependent, structures to the small scales where dissipation into heat is observed. With the emergence of simulation techniques based on scale separation, such as the large-eddy simulations (LES) [5, 6], these studies have also acquired a more applied flavour. Indeed, in LES, the small scales are not captured by the numerical grid and their influence on the large scale flow has to be modelled. Since their major effect is to pump energy, the knowledge of this energy transfer is essential to design accurate small scale models.

When the fluid is electrically conducting, the Navier–Stokes equation has to be coupled to an induction equation for the magnetic field, yielding the magnetohydrodynamics (MHD) equations. The analysis of energy transfers in MHD has closely followed the pioneering works on fluid turbulence [7] and is still a very active field of research [8–10]. The extension of LES to magnetohydrodynamics [11–13] motivates further the research in this field and the present study aims at contributing to it. High resolution (512^3) direct numerical simulations (DNS) of forced MHD turbulence have been performed and the velocity and magnetic fields have been analysed using a shell decomposition. The energy exchanges between different

*Corresponding author. E-mail: dcarati@ulb.ac.be

Journal of Turbulence
ISSN: 1468-5248 (online only) © 2006 Taylor & Francis
http://www.tandf.co.uk/journals
DOI: 10.1080/14685240600774017

scales are characterized by shell-to-shell transfers. Moreover, two different strategies to split these energy exchanges into forward and backward contributions are proposed.

The analysis is also extended to the MHD equations reformulated in terms of the Elsässer variables [14]. The number of nonlinear terms then appears to be reduced and the energy transfers are simpler as a consequence of the separated energy conservation for each of the Elsässer variables. This may provide some motivation for re-expressing the LES models for MHD in terms of the Elsässer variables, at least when the Prandtl number is not too far from unity.

2. Shell decomposition

The MHD equations resulting from the coupling between hydrodynamics and electromagnetisms are well known. In this paper, we consider incompressible MHD for which the evolution equations for the velocity and magnetic fields read

$$\partial_t u_i = -u_j \partial_j u_i + b_j \partial_j b_i - \partial_i p + f_i + \nu \nabla^2 u_i, \tag{1}$$

$$\partial_t b_i = -u_j \partial_j b_i + b_j \partial_j u_i + \eta \nabla^2 b_i. \tag{2}$$

In these equations, f_i is an external mechanical force, ν is the kinematic viscosity, p is the total (hydrodynamic + magnetic) pressure divided by the fluid density, which is assumed to be constant. In that case, both the magnetic and velocity fields are divergence free $\partial_l u_l = 0 = \partial_l b_l$. The magnetic field is rescaled using Alfvén's units and has the dimensions of a velocity. In the examples treated below, the magnetic diffusivity η will be chosen to be equal to the viscosity, so that the magnetic Prandtl number is unity.

Details on the direct numerical simulations (DNS) of equations (1) and (2), which are performed using a Fourier representation of u_i and b_i, are given in the next section. Several velocity and magnetic fields obtained in these DNS have been analysed in detail by using a shell variable decomposition. The Fourier space is divided into spherical shells s_n that contain all the wave vectors such that $k_n \leq ||\vec{k}|| < k_{n+1}$. The velocity field obtained by keeping all the Fourier modes in the shell s_n while setting to 0 the modes outside this shell is denoted by $\vec{u}_n(\vec{k})$. Its inverse Fourier transform, $\vec{u}_n(\vec{r})$, can be used to give a physical space representation of the shell velocity. Similarly, magnetic field shell variables may be defined, and kinetic and magnetic shell energies are given by the following expressions:

$$E_n^u = \frac{1}{2} \sum_{\vec{k} \in s_n} |\vec{u}(\vec{k})|^2 = \frac{1}{2} \sum_{\vec{k}} |\vec{u}_n(\vec{k})|^2 = \frac{1}{2} \int \mathrm{d}\vec{r}\ \vec{u}_n(\vec{r})^2, \tag{3}$$

$$E_n^b = \frac{1}{2} \sum_{\vec{k} \in s_n} |\vec{b}(\vec{k})|^2 = \frac{1}{2} \sum_{\vec{k}} |\vec{b}_n(\vec{k})|^2 = \frac{1}{2} \int \mathrm{d}\vec{r}\ \vec{b}_n(\vec{r})^2. \tag{4}$$

The spectral energy density associated with the shell variable $\vec{u}_n(\vec{k})$ is thus a function that has a compact support in the Fourier space restricted to a shell. However, in the physical space this energy density is not localized and clearly exhibits structures that have a typical length scale of the order of $\ell_n = k_n^{-1}$ as shown in figure 1. The evolution of the shell energies is given by the following coupled equations:

$$\partial_t E_n^u = \sum_m T_{n,m}^{u,u} + \sum_m T_{n,m}^{u,b} + F_n^u - D_n^u, \tag{5}$$

$$\partial_t E_n^b = \sum_m T_{n,m}^{b,u} + \sum_m T_{n,m}^{b,b} - D_n^b, \tag{6}$$

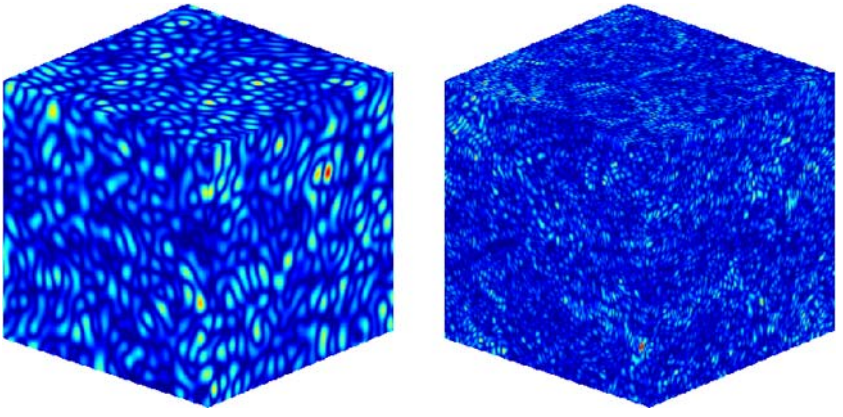

Figure 1. Physical space energy density of the shell velocity variable $\vec{u}_6(\vec{r})$ (left) and $\vec{u}_{12}(\vec{r})$ (right).

where F_n^u is the shell energy injected per unit of time due to external mechanical forcing terms (there is no such forcing terms in the magnetic field equation), while D_n^u and D_n^b are respectively the kinematic and the magnetic energy dissipation rates:

$$F_n^u = \sum_{\vec{k}} \mathrm{Re}\{\vec{u}_n(\vec{k}) \cdot \vec{f}(\vec{k})^*\} \tag{7}$$

$$D_n^u = \nu \sum_{\vec{k}} k^2 |\vec{u}_n(\vec{k})|^2 \tag{8}$$

$$D_n^b = \eta \sum_{\vec{k}} k^2 |\vec{b}_n(\vec{k})|^2, \tag{9}$$

where Re represents the real part of a complex number. The shell-to-shell energy transfers are given by

$$T_{n,m}^{u,u} = -\sum_{\vec{k}\in s_n} \sum_{\vec{p}\in s_m} \mathrm{Im}\{\vec{k} \cdot \vec{u}(\vec{k}+\vec{p})^* \, \vec{u}(\vec{p}) \cdot \vec{u}(\vec{k})\} \tag{10}$$

$$T_{n,m}^{u,b} = +\sum_{\vec{k}\in s_n} \sum_{\vec{p}\in s_m} \mathrm{Im}\{\vec{k} \cdot \vec{b}(\vec{k}+\vec{p})^* \, \vec{b}(\vec{p}) \cdot \vec{u}(\vec{k})\} \tag{11}$$

$$T_{n,m}^{b,u} = +\sum_{\vec{k}\in s_n} \sum_{\vec{p}\in s_m} \mathrm{Im}\{\vec{k} \cdot \vec{b}(\vec{k}+\vec{p})^* \, \vec{b}(\vec{p}) \cdot \vec{u}(\vec{k})\} \tag{12}$$

$$T_{n,m}^{b,b} = -\sum_{\vec{k}\in s_n} \sum_{\vec{p}\in s_m} \mathrm{Im}\{\vec{k} \cdot \vec{u}(\vec{k}+\vec{p})^* \, \vec{b}(\vec{p}) \cdot \vec{b}(\vec{k})\} \tag{13}$$

where Im represents the imaginary part of a complex number and the symbol * represents the complex conjugate of a complex number. In the DNS results analysed in the next sections, forced turbulence is simulated using a force that is limited to one shell of wave vector s_f (typically $s_f = s_4$, so that energy is injected only at large scales). All modes in the shell s_f are submitted to a force defined by

$$\vec{f}(\vec{k}) = \alpha \frac{\vec{u}(\vec{k})}{|\vec{u}(\vec{k})|^2}, \tag{14}$$

where $\alpha = \epsilon / N_f$ is the ratio between the desired total energy injection rate ϵ and the number of modes N_f in the forcing shell s_f. This forcing is very similar to the one introduced in [15].

Considering expressions (7) and (14), it is easy to show that such a forcing mechanism injects a constant rate of energy ϵ in the flow. The forcing and dissipation mechanisms do not couple the different shell energies and they are defined for each shell independently. However, the terms $T^{x,y}_{n,m}$ where x and y can be either u or b correspond to energy transfers between different shell variables and have to satisfy the following properties that derive directly from energy conservation in the limit of vanishing forcing and dissipation:

$$T^{x,y}_{n,m} = -T^{y,x}_{m,n}. \tag{15}$$

The explicit mathematical form of these energy transfers $T^{x,y}_{n,m}$ can be derived straightforwardly from equations (1) and (2) and has been discussed in many papers [2, 4]. Before presenting the DNS analysis of the shell energy transfers, it is interesting to rewrite equations (1) and (2) in terms of the Elsässer variables $z^{\pm}_i = u_i \pm b_i$:

$$\partial_t z^{\pm}_i = -z^{\mp}_j \partial_j z^{\pm}_i - \partial_i p + f_i + \nu^{\pm}\nabla^2 z^{\pm}_i + \nu^{\mp}\nabla^2 z^{\mp}_i, \tag{16}$$

where $\nu^{\pm} = (\nu \pm \eta)/2$. Contrary with the kinetic or the magnetic energies, the energies associated with the Elsässer variables are conserved separately by the nonlinear terms as a consequence of the total energy conservation and the cross helicity ($\vec{u} \cdot \vec{b}$) conservation. A shell decomposition for the Elsässer variables can also be considered and the related shell energy equations read

$$\partial_t E^{+}_n = \sum_m T^{+,+}_{n,m} + F^{+}_n - D^{+}_n, \tag{17}$$

$$\partial_t E^{-}_n = \sum_m T^{-,-}_{n,m} + F^{-}_n - D^{-}_n, \tag{18}$$

where

$$F^{\pm}_n = \sum_{\vec{k}} \mathrm{Re}\{\vec{z}^{\pm}_n(\vec{k}) \cdot \vec{f}(\vec{k})\} \tag{19}$$

$$D^{\pm}_n = \sum_{\vec{k}} k^2(\nu^{\pm} |\vec{z}^{\pm}_n(\vec{k})|^2 + \nu^{\mp}\mathrm{Re}\{\vec{z}^{+}_n(\vec{k}) \cdot \vec{z}^{-}_n(\vec{k})\}) \tag{20}$$

$$T^{+,+}_{n,m} = -\sum_{\vec{k}\in s_n} \sum_{\vec{p}\in s_m} \mathrm{Im}\{\vec{k} \cdot \vec{z}^{-}(\vec{k}+\vec{p})^* \vec{z}^{+}(\vec{p}) \cdot \vec{z}^{+}(\vec{k})\} \tag{21}$$

$$T^{-,-}_{n,m} = -\sum_{\vec{k}\in s_n} \sum_{\vec{p}\in s_m} \mathrm{Im}\{\vec{k} \cdot \vec{z}^{+}(\vec{k}+\vec{p})^* \vec{z}^{-}(\vec{p}) \cdot \vec{z}^{-}(\vec{k})\}. \tag{22}$$

As a consequence of the conservation of the Elsässer variable energies, the shell-to-shell energy transfers, schematically represented in figure 2, do not couple the two variables and this simplifies strongly the analysis. It should be noted however that the kinetic and magnetic energies cannot be derived from the knowledge of the Elsässer energies. As a consequence, the transfers $T^{x,y}_{n,m}$ appearing in equations (5) and (6) cannot be derived from the knowledge of $T^{+,+}_{n,m}$ and $T^{-,-}_{n,m}$. Similarly, the shell-to-shell transfers (21) and (22) for the Elsässer variables cannot be derived from the shell-to-shell transfers for the velocity and magnetic fields (10)–(13). This can be understood easily since the expansion of $T^{+,+}_{n,m}$ and $T^{-,-}_{n,m}$ in terms of $\vec{u}$ and $\vec{b}$ will show cubic terms in $\vec{b}$ that do not enter the definition of the transfers (10)–(13).

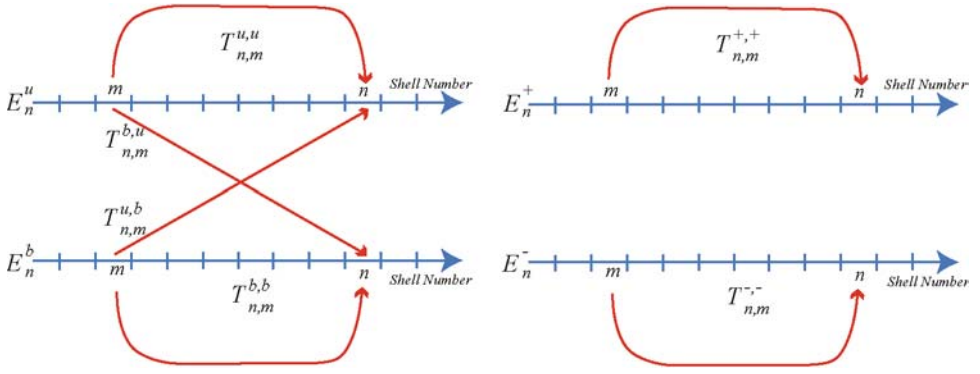

Figure 2. Schematic representation of the shell-to-shell energy transfers between velocity and magnetic field variables (left) and between the Elsässer variables (right).

3. DNS analysis

Equations (1) and (2) have been solved numerically in a cubic box whose size is $L = 2\pi$ using a fully dealiased pseudo-spectral code. The dissipative linear terms proportional to ν and η are treated analytically using exponential factors, so that the time step can be computed automatically using a CFL criterion only. A third-order Runge–Kutta method is implemented for the time advancement. The Reynolds number R_λ (based on Taylors micro-scale) for the initial field is about 180. The number of grid points is 512^3 and the product of the Kolmogorov length $\ell_\nu = (\nu^3/\epsilon)^{1/4}$ and the maximal wavenumber $k_{\max} = 256$ is larger than 1.6. Here ϵ is computed as the instantaneous total kinetic + magnetic dissipation.

After a transient time, the total dissipation appears to fluctuate around the imposed energy injection rate that enters the forcing definition (14). As a consequence, the Kolmogorov length is indirectly imposed by the run parameters. Another advantage of the forcing is that it may be easily modified to inject simultaneously kinetic energy and kinetic helicity by adding a term proportional to the vorticity. In its present form, no kinetic helicity is injected and several runs show that, even if present under the initial conditions, kinetic helicity tends to decay. Similarly, the cross helicity normalized by the total energy,

$$\sigma_c = \frac{2\vec{u}\cdot\vec{b}}{\vec{u}^2 + \vec{b}^2}, \tag{23}$$

remains very small ($|\sigma_c| \lesssim 0.02$) as well as the normalized magnetic helicity defined by

$$\sigma_m = \frac{\vec{a}\cdot\vec{b}}{\int \mathrm{d}k\; k^{-1} E^b(k)}, \tag{24}$$

which is less than 1% where $\vec{b} = \nabla \times \vec{a}$ and $E^b(k)$ is the magnetic energy spectrum. The forcing is acting in the range $[k_{\inf} = 1.5, k_{\sup} = 3.1]$. This range contains 104 modes so that the energy injected is equidistributed amongst a fairly large number of modes, ensuring isotropy even at large scales. The energy spectra produced by this forcing are presented in figure 3.

In the shell decomposition of the DNS data, the shell boundaries k_n are chosen to grow algebraically $k_{n+1} = gk_n$ with $g = 2^{1/4}$ between $n = 4$ and $n = 19$. The first k_n's have been chosen differently ($k_1 = 0$, $k_2 = 2$, $k_3 = 4$ and $k_4 = 8$) in order to ensure that enough modes

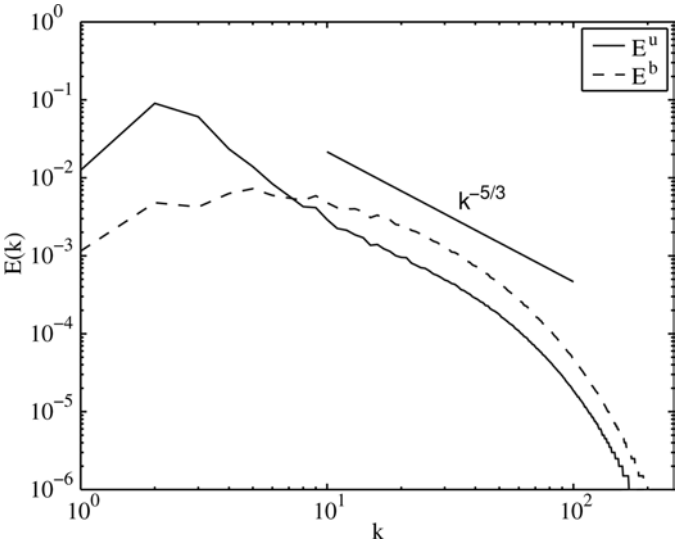

Figure 3. Kinetic and magnetic energy spectra.

belong to the first three shells. Also, in order to limit the number of shells, the last shell s_{20}, which entirely lies in the dissipation range, is wider and limited by $k_{20} = 128$ and $k_{21} = 256$.

3.1 *Shell-to-shell transfers*

The shell-to-shell energy transfers are conveniently analysed using a two-dimensional representation as in figure 4. First results for decaying MHD turbulence have been reported elsewhere [23], so that the present discussion will focus mainly on the analysis of the forced MHD turbulence DNS. The sign of the shell-to-shell energy transfers is not prescribed and, as a consequence of the total energy conservation, $T^{x,y}_{n,m}$ have to sum up to 0. If $T^{x,y}_{n,m}$ is positive, the shell variable x_n is receiving energy from the shell variable y_m. The symmetry relation (15) automatically implies that, in this case, the shell variable y_m is losing energy at the expense of shell variable x_m. When $T^{x,y}_{n,m}$ is positive for $n > m$, the situation is referred to as a 'forward' energy transfer. Otherwise, it is referred to as a 'backward' energy transfer. When the largest (positive as well as negative) value of $T^{x,y}_{n,m}$ is observed for n close to m, the energy transfer is referred to as 'local'. It is important to realize that the locality of the energy transfer has to be interpreted as energy exchanges between structures that have similar length scales and not necessarily between positions that are close to each other in the physical space.

As expected from the phenomenology of turbulence, the energy transfers $T^{u,u}_{n,m}$ and $T^{b,b}_{n,m}$ are essentially local and forward. This can be seen in figure 4. Locality can be observed since all the significant transfers are along the diagonal where n is close to m. Only direct transfers are observed which is confirmed by the positive value below the diagonal and the negative value above. Also, scale independent energy transfers can be observed since all the horizontal lines are very much similar when properly shifted by m boxes, i.e. $T^{a,b}_{n,m}$ is essentially a function of $n - m$ and not of n and m separately. Such properties confirm previous results obtained for decaying turbulence.

These properties also support the use of shell models for investigating the dynamics of turbulent systems. Indeed, shell models strongly rely on the locality as well as the scale invariance of the turbulent interactions. In these models, the hydrodynamic or magnetohydrodynamic

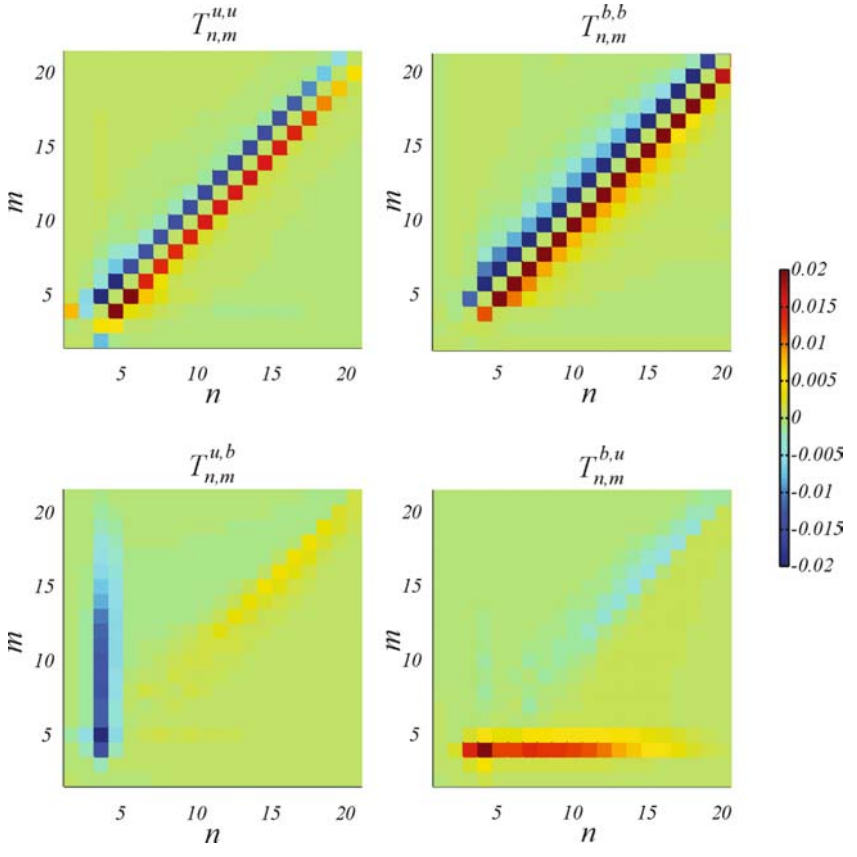

Figure 4. Two-dimensional representation of the shell-to-shell energy transfers. The horizontal coordinate corresponds to the receiving shell and the vertical coordinate to the giving shell.

equations are replaced by a set of ordinary differential equations for a small number of complex variables, each of which is summarizing the total information from a shell of wave vectors. As in the present analysis, these variables are associated with wave numbers that grow algebraically $k_i = k_{i-1}\, g$. In shell models, the parameter g is usually assumed to be 2 and the shell variable interactions are limited to the first two neighbour shells. This choice however largely covers the interactions observed from the analysis of the DNS presented in figure 4 where the shells are much thinner ($g = 2^{1/4}$). These shell models have been originally proposed for Navier–Stokes turbulence [16–18] and later extended to MHD [19–21] as well as to MHD with passive scalar [22]. The analysis of shell-to-shell energy transfers in a shell model simulation would be much simpler than for a DNS since mode-to-mode interactions would almost coincide with the shell-to-shell energy transfers. Such a study is beyond the scope of our work but would be an interesting extension to the present analysis.

The results are however different for the $T^{u,b}_{n,m}$ and $T^{b,u}_{n,m}$ energy transfers (which are not independent as a consequence of the property (15)). Indeed, a strong non-local contribution from the forced velocity shell to all the magnetic shells is observed. This also confirms previous results obtained using different forcing mechanisms [24–26] which, contrary to the forcing (14), generate an average velocity field. Hence, this phenomenon of distant interactions between the velocity and the magnetic fields in forced turbulence appears to be independent of the type of forcing. The analysis of the Elsässer shell transfers shows that both these features

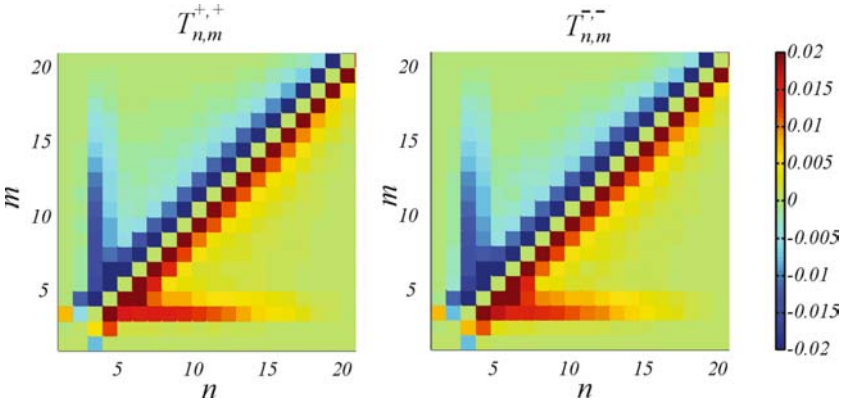

Figure 5. Two-dimensional representation of the shell-to-shell energy transfers between the Elsässer variables in forced MHD turbulence.

of local and forward transfer and non-local transfer from the forced shell are combined in $T^{+,+}_{n,m}$ and $T^{-,-}_{n,m}$. This is not a surprise since the Elsässer variables mix u_i and b_i. Moreover, the two quantities $T^{+,+}_{n,m}$ and $T^{-,-}_{n,m}$ are very similar. Actually, they are given by sums which are strongly dominated by the same terms. The remaining terms are different but with relatively small amplitudes. This explains why the two representations in figures 5 are almost indistinguishable.

3.2 *Forward and backward transfers*

In turbulence, all the modes are coupled as a result of the nonlinearities. For instance, the shell-to-shell energy transfer $T^{u,b}_{n,m}$ thus corresponds to a large number of mode-to-mode interactions in which three modes are involved: a 'receiving' mode $\vec{u}(\vec{k})$ from the shell variable $\vec{u}_n$ (i.e. $\vec{k} \in s_n$), a 'giving' mode $\vec{b}(\vec{p})$ from the shell variable $\vec{b}_m$ (i.e. $\vec{p} \in s_m$) and a 'mediator' mode that can belong to any shell. The mediator mode is however entirely determined by the constraint $\vec{k} + \vec{p} + \vec{q} = 0$. These three mode interactions are usually referred to as triads. Obviously, the fact that a given shell-to-shell transfer $T^{u,b}_{n,m}$ is positive does not imply that all the triad interactions correspond to a positive energy transfer from $\vec{b}(\vec{p})$ to $\vec{u}(\vec{k})$.

In a previous study [23], the shell-to-shell transfers have been separated into positive $T^{u,b}_{n,m,(+)}$ and negative $T^{u,b}_{n,m,(-)}$ contributions. This decomposition is however not unique and two different definitions have been chosen. In the first one, the positive transfer, denoted as $T^{u,b,(+)}_{n,m,(k)}$, is defined by the sum of all the triads interaction for which $\vec{b}_m$ loses energy and $\vec{u}_n$ gains energy. In another decomposition, the positive transfer, denoted as $T^{u,b,(+)}_{n,m,(r)}$, is defined using the physical space shell variable and, roughly speaking, corresponds to all the locations for which $\vec{u}_n(\vec{r})$ gains energy. Independently of the decomposition, the following relations should be satisfied:

$$T^{x,y,(+)}_{n,m} \geq 0, \tag{25}$$

$$T^{x,y,(-)}_{n,m} \leq 0, \tag{26}$$

$$T^{x,y,(+)}_{n,m} = -T^{y,x,(-)}_{m,n}, \tag{27}$$

$$T^{x,y}_{n,m} = T^{x,y,(+)}_{n,m} + T^{x,y,(-)}_{n,m}. \tag{28}$$

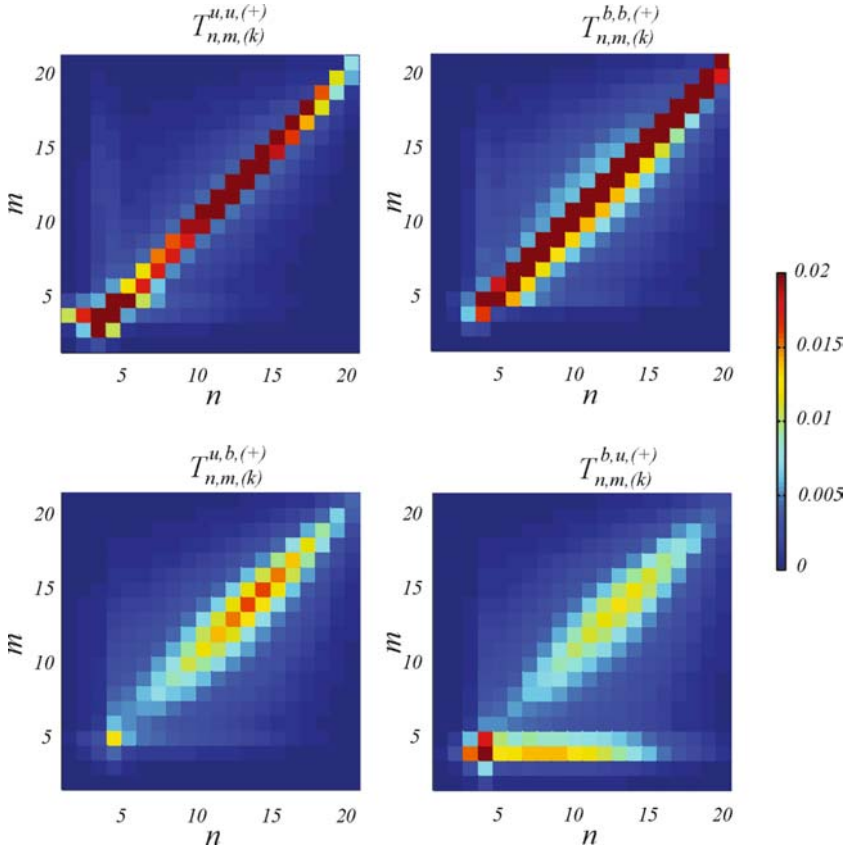

Figure 6. Two-dimensional representation of the positive parts of the energy transfers defined using the Fourier space representation ($T^{x,y,(+)}_{n,m,(k)}$).

It is important to note that nothing guarantees the equivalence of the different decomposition into positive and negative contributions and, in particular, it has been shown that

$$T^{x,y,(+)}_{n,m,(r)} \neq T^{x,y,(+)}_{n,m,(k)}. \tag{29}$$

This difference can be seen by comparing figures 6 and 7. While the transfers $T^{x,y,(+)}_{n,m,(k)}$ are very much local (no strong contribution for large values of $n - m$), the situation is quite different for the transfers $T^{x,y,(+)}_{n,m,(r)}$, which appear to be strongly non-local. This striking difference may be due to the choice of the spectral definition of the shell variables and other decompositions of the total fields into subsets might lead to results much more independent of the definition of positive and negative energy transfers.

The same decomposition between positive and negative contribution can obviously also be performed for the Elsässer variables. Figure 8 shows the results for the Fourier space decomposition. The positive transfer $T^{+,+,(+)}_{n,m,(k)}$ and $T^{-,-,(+)}_{n,m,(k)}$ seem to be globally less local, though the non-local transfer from the forced shell is less marked than in figure 5. Again, $T^{+,+,(+)}_{n,m,(k)}$ and $T^{-,-,(+)}_{n,m,(k)}$ are almost indistinguishable.

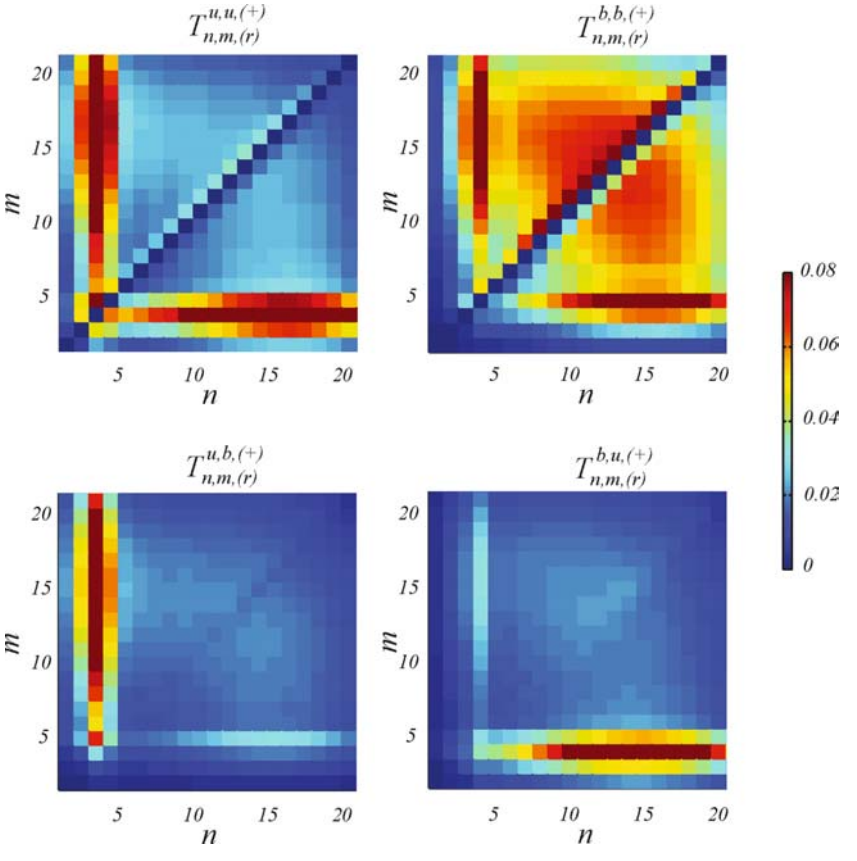

Figure 7. Two-dimensional representation of the positive parts of the energy transfers defined using the physical space representation ($T^{x,y,(+)}_{n,m,(r)}$).

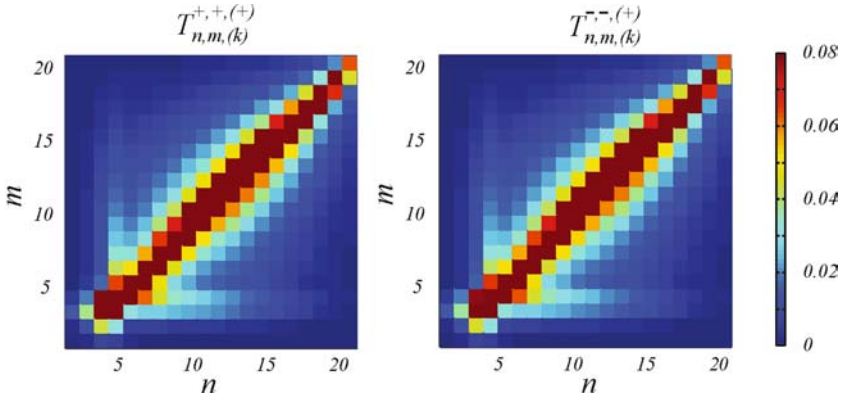

Figure 8. Two-dimensional representation of the positive parts of the energy transfers between the Elsässer shell variables defined using the Fourier space representation.

4. Conclusion

DNS databases of forced isotropic MHD turbulence are analysed using a shell decomposition of the velocity and magnetic fields. The kinetic and magnetic energy cascades are essentially forward and local, although a non-local transfer of energy between the forced velocity shell and the small scale magnetic field is observed. This non-local transfer seems to be independent of the forcing mechanism since it has also been observed in previous studies [24–26] where different mechanical forces were used. In particular, in [24, 25, 26], the forcing mechanism is constant (infinite time correlation) and generates an averaged large scale flow. It is thus interesting to note that the same non-local energy transfer is observed with the forcing (14) that has a finite time correlation and preserves isotropy even at large scales. It is also worth mentioning that such a non-local energy transfer is not observed in the decaying turbulence simulation [23]. This is actually the major observed difference in the energy transfers between decaying and forced turbulence.

The shell variable decomposition has been extended to the Elsässer variables. Again, the global picture seems to be the superposition of mostly forward and local cascades and non-local interactions between the forced shell and all the other shells. The fact that the Elsässer variables exhibit basically the same type of energy exchanges is expected but not necessarily trivial. Indeed, the shell-to-shell energy transfers in the Elsässer formulation cannot be derived from those computed in the velocity–magnetic fields formulation. The present analysis suggests that it might be interesting to explore the LES modelling in terms of the Elsässer variables. Indeed, the number of nonlinearities in the Elsässer equations is reduced when compared to the velocity–magnetic field equations ((2) instead of (4)), so that less subgrid scale stress tensors do require a modelling effort. Moreover, the Elsässer shell-to-shell interactions do not seem to be more complex. There is thus a hope that simple traditional models (such as eddy viscosity and eddy magnetic diffusivity models expressed for the Elsässer variables) would be well adapted to the Elsässer formulation and less demanding than in the velocity–magnetic field formulation.

The shell-to-shell energy transfers have been further decomposed into forward and backward contributions using two different strategies. The results are very different and show that the interpretation of backscatter [15, 27, 28] (the backward energy transfer) is closely linked to the definition of the scale separation. As a consequence, the design of LES models that could account for the dissipative effects of the small scales as well as for the large-scale energy feeding by small structures will depend on the very nature of the separation into resolved and unresolved scales.

Acknowledgements

This work has been supported by the Fonds National pour la Recherche Scientifique (Belgium, FRFC 2.4542.05), the Fonds Defay, the Communauté Française de Belgique (ARC 02/07-283) and the contract of association EURATOM—Belgian state. The content of the publication is the sole responsibility of the authors and it does not necessarily represent the views of the Commission or its services.

References

[1] Kraichnan, R., 1971, Inertial-range transfer in two and three-dimensional turbulence. *Journal of Fluid Mechanics*, **47**, 525–535.

[2] Domaradski, J.A. and Rogallo, R.S., 1990, Local energy-transfer and nonlocal interactions in homogeneous, isotropic turbulence. *Physics of Fluids A*, **2**, 413–426.
[3] Zhou, Y., 1993, Degrees of locality of energy transfer in the inertial range. *Physics of Fluids A*, **5**, 1092–1094.
[4] Kerr, R.M., Domaradzki, J.A. and Barbier, G., 1996, Small-scale properties of nonlinear interactions and subgrid-scale energy transfer in isotropic turbulence. *Physics of Fluids*, **8**, 197–208.
[5] Rogallo, R. and Moin, P., 1984, Numerical simulation of turbulent flows. *Annual Reviews of Fluid Mechanics,* **16**, 99–137.
[6] Ghosal, S. and Moin, P., 1995, The basic equations for large eddy simulation of turbulent flows in complex geometries *Journal of Computational Physics*, **118**, 24–37.
[7] Pouquet, A., Frisch, U. and Léorat J., 1976, Strong MHD helical turbulence and the non–linear dynamo effect, *Journal of Fluid Mechanics*, **77**, 321–354.
[8] Dar, G., Verma, M. and Eswaran, V., 2001, Energy transfer in two-dimensional magnetohydrodynamic turbulence: formalism and numerical results. *Physica D*, **3**, 207–225.
[9] Schilling, O. and Zhou, Y., 2002, Triadic energy transfers in non-helical magnetohydrodynamic turbulence. *Journal of Plasma Physics*, **68**, 389–406.
[10] Verma, M.K., 2004, Statistical theory of magnetohydrodynamic turbulence: recent results. *Physics Report*, **401**, 229–380.
[11] Yoshizawa, A., 1987, Subgrid modeling for magnetohydrodynamic turbulent shear flows. *Physics of Fluids*, **30**, 1089–1095.
[12] Theobald, M., Fox, P. and Sofia, S., 1994, A subgrid-scale resistivity for magnetohydrodynamics. *Physics of Plasmas*, **1**, 3016.
[13] Agullo, O., Muller, W.-C., Knaepen, B. and Carati, D., 2001, Large eddy simulation for decaying magnetohydrodynamics turbulence with dynamic subgrid modelling. *Physics of Plasmas*, **7**, 3502–3505.
[14] Elsässer, W. M., 1950, The hydromagnetic equations. *Physical Review*, **79**, 183–183.
[15] Carati, D., Ghosal, S. and Moin, P., 1995, On the representation of backscatter in dynamic localization models. *Physics of Fluids*, **7**, 606–616.
[16] Gledzer, E. B., 1973, System of hydrodynamic type admitting two quadratic integrals of motion. *Soviet Physics Doklady*, **18**, 216–217.
[17] Ohkitani, K. and Yamada, M., 1990, Enstrophy cascade in a model of 2D turbulence. *Progress of Theoretical Physics*, **84**, 415–419.
[18] Biferale, L., 2003, Shell models of energy cascade in turbulence. *Annual Review of Fluid Mechanics*, **35**, 441–468.
[19] Gloaguen, C., Léorat, J., Pouquet, A. and Grappin, R., 1985, A scalar model for MHD turbulence. *Physica D,* **170**, 154–182.
[20] Biskamp, D., 1994, Cascade models for magnetohydrodynamic turbulence *Physical Review E*, **50**, 2702–2711.
[21] Frick, P. and Sokoloff, D., 1998, Cascade and dynamo action in a shell model of magnetohydrodynamic turbulence *Physical Review E*, **57**, 4155–4164.
[22] Gilbert, T. and Mitra, S., 2004, Statistics of active versus passive advections in magnetohydrodynamic turbulence. *Physical Review E*, **69**, 057301.
[23] Debliquy, O., Verma, M.K. and Carati, D., 2005, Energy fluxes and shell-to-shell transfers in three-dimensional decaying magnetohydrodynamic turbulence. *Physics of Plasmas*, **12**, 042309.
[24] Alexakis, A., Mininni, P.D. and Pouquet, A., 2005, Imprint of large-scale flows on turbulence. *Physical Review Letters*, **95**, 264503.
[25] Alexakis, A., Mininni, P.D. and Pouquet, A., 2005, Shell-to-shell energy transfer in magnetohydrodynamics: I. Steady state turbulence. *Physical Review E*, **72**, 046301.
[26] Mininni, P.D., Alexakis, A. and Pouquet, A., 2005, Shell-to-shell energy transfer in magnetohydrodynamics: II. Kinematic dynamo. *Phys. Rev. E,* **72**, 046302.
[27] Leith, C.E., 1990, Stochastic backscatter in a subgrid-scale model: plane shear mixing layer. *Physics of Fluids A*, **2**, 297–299.
[28] Mason, P.J. and Thomson, D.J., 1992, Stochastic backscatter in large-eddy simulations of boundary layers. *Journal of Fluid Mechanics*, **242**, 51–78.